Accepted Manuscript

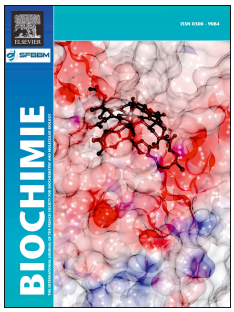

Selection and characterization of DNA aptamers for detection of glutamate dehydrogenase from *Clostridium difficile*

Meng Liu, Qingxin Yin, John D. Brennan, Yingfu Li

PII: S0300-9084(17)30224-9

DOI: 10.1016/j.biochi.2017.08.015

Reference: BIOCHI 5263

To appear in: *Biochimie*

Received Date: 14 July 2017

Accepted Date: 31 August 2017

Please cite this article as: M. Liu, Q. Yin, J.D. Brennan, Y. Li, Selection and characterization of DNA aptamers for detection of glutamate dehydrogenase from *Clostridium difficile*, *Biochimie* (2017), doi: 10.1016/j.biochi.2017.08.015.

Rapid and accurate diagnosis of *Clostridium difficile* infections (CDI) is crucial for patient treatment, infection control and epidemiological monitoring. As an important antigen, glutamate dehydrogenase (GDH) has been proposed as a preliminary screening test target for CDI. However, current assays based on GDH activity or GDH immunoassays have suboptimal sensitivity and specificity. To overcome these limitations, it is urgent to explore new biomolecular recognition and detection methods for CDI detection. Herein, we describe the selection and characterization of single-stranded DNA aptamers that specifically targeted GDH. After 10 rounds of selection, high-throughput sequencing was used to identify enriched aptamer candidates. Of 10 candidates, three aptamers for GDH were identified. Gel shift assays showed that these aptamers exhibited low nanomolar affinities. One aptamer was optimized based on structural analysis and further engineered into a structure-switching fluorescence signaling aptamer, wherein desorption from reduced graphene oxide (RGO) upon binding of GDH led to an increase in fluorescence emission. This method allowed for quantitative detection of GDH with a detection limit of 1 nM, providing great potential for its further application in CDI diagnosis.

Selection and Characterization of DNA Aptamers for Detection of Glutamate Dehydrogenase from *Clostridium difficile*

Meng Liu,[†,‡,§] Qingxin Yin,[§] John D. Brennan*[†,‡] and Yingfu Li*[,†,‡]

[†]Department of Biochemistry and Biomedical Sciences and Chemistry and Chemical Biology, McMaster University, 1280 Main Street West, Hamilton, ON, L8S 4K1 (Canada).

[‡]Biointerfaces Institute, McMaster University, 1280 Main Street West, Hamilton, ON, L8S A03 (Canada).

[§]School of Environmental Science and Technology, Key Laboratory of Industrial Ecology and Environmental Engineering (Ministry of Education), Dalian University of Technology, Dalian, 116024 (China).

*Correspondence: liying@mcmaster.ca or brennanj@mcmaster.ca

ABSTRACT. Rapid and accurate diagnosis of *Clostridium difficile* infections (CDI) is crucial for patient treatment, infection control and epidemiological monitoring. As an important antigen, glutamate dehydrogenase (GDH) has been proposed as a preliminary screening test target for CDI. However, current assays based on GDH activity or GDH immunoassays have suboptimal sensitivity and specificity. Herein, we described the selection and characterization of single-stranded DNA aptamers that specifically targeted GDH. After 10 rounds of selection, high-throughput sequencing was used to identify enriched aptamer candidates. Of 10 candidates, three aptamers for GDH were identified. Gel shift assays showed that these aptamers exhibited low nanomolar affinities. One aptamer was optimized based on structural analysis and further engineered into a structure-switching fluorescence signaling aptamer, wherein desorption from reduced graphene oxide (RGO) upon binding of GDH led to an increase in fluorescence emission. This method allowed for quantitative detection of GDH with a detection limit of 1 nM, providing great potential for its further application in CDI diagnosis.

Keywords

Aptamer; in vitro selection; biosensor; *Clostridium difficile*; glutamate dehydrogenase; graphene oxide

1. Introduction

In recent years, outbreaks of healthcare-associated infections resulting from toxin-producing *Clostridium difficile* (*C. difficile*) have been widespread and are associated with increased morbidity and mortality. *C. difficile* is responsible for 90-100% of cases of pseudomembranous colitis, 15-25% of antibiotic-associated diarrheas and 60-75% of antibiotic-associated colitis [1-4]. According to a recent Canadian study, the incidence of *C. difficile* infection (CDI) in Canada is 65 CDI cases per 100,000 patient-days for adult patients admitted to hospitals, accompanied with a mortality rate of 5.7% [5]. In the United States, about 15,000-20,000 patients die annually from CDI [6]. Furthermore, the economic burden for taking care of CDI patients is significant: a hospital-acquired CDI increases the cost of otherwise matched hospitalizations by 4-fold, translating to over $1 billion in added cost annually [7]. A key to reducing the negative outcomes of CDI is rapid and accurate diagnosis so that the treatment of patients can be quickly implemented and the nosocomial spread of these infections effectively controlled.

Traditionally, CDI can be diagnosed using the cell cytotoxicity neutralization assay, which detects the presence of toxin, and is often considered to be the clinical gold standard for the detection of *C. difficile* from fecal samples [8]. This method performs with superior sensitivity but is labor-intensive, time consuming (up to 4 days) and requires skilled technicians [9,10]. Since the pathogenicity of *C. difficile* is linked to the two large toxins, toxin A and toxin B, toxin enzyme immunoassays (EIAs) have proven to be a significant advancement. These assays are technically simple, fast and frequently used as stand-alone assays, but have low sensitivity [11], which results in poor positive predictive values if the prevalence of TcdA/B in stool samples is relatively low (< 10%) [12]. Alternatively, the direct detection of genes encoding toxin A and/or toxin B has become a diagnostic target using polymerase chain reaction (PCR) technology. The main advantages of these molecular assays are high sensitivity and relatively short turnaround time [13]. However, several drawbacks, including intensive sample preparation, cost and potential for error limit their clinical utility [14].

Recently, significant effort has been focused on the detection of a so-called common antigen for CDI, the glutamate dehydrogenase (GDH) enzyme, which is highly conserved and commonly produced by most isolates of *C. difficile* in large amounts [15,16]. Although GDH assays cannot discriminate between toxigenic and nontoxigenic strains, these assays have been proposed as initial screening tools for *C. difficile* in stool samples due to their high negative predictive values (>99%) [14,17,18]. To improve the accuracy and efficiency of CDI diagnosis, two-step or three-step testing algorithms have been utilized involving a preliminary screening *via* GDH assay followed by a confirmatory test for positive samples using the cell cytotoxin assay, EIAs or PCR for TcdA/B [14,19,20]. For example, the Society for Healthcare Epidemiology of America (SHEA) and the Infectious Diseases Society of America (IDSA) guidelines recommend such a two-step algorithm using EIAs for GDH as an initial screening and then the cell cytotoxicity assay or toxigenic culture as the confirmatory test for GDH-positive stool samples [21]. In view of the role of GDH as a universal CDI marker, we can conclude that it is critical to develop a rapid, sensitive, accurate and cost-effective method for detection of GDH as a key step in diagnosing CDI.

To date, the most commonly used tests for GDH are EIAs, which can provide rapid results, but demonstrate suboptimal clinical sensitivity, ranging from 79.2% to 98%, which varies significantly with the prevalence of CDI [15,22,23]. Furthermore, antibodies against GDH could cross-react with GDH produced by other anaerobic bacteria such as *Clostridium sporogenes*, *Peptostreptococcus anaerobius* and *Clostridium botulinum* [24]. In addition, the limited stability and high cost of antibodies remain as challenges. To overcome these limitations, it is urgent to explore new biomolecular recognition and detection methods for CDI detection. Nucleic acid aptamers are synthetic single-stranded DNA or RNA molecules with a defined tertiary structure that can selectively bind to a target of interest. Remarkable progress has been made in aptamer research since the report of the first aptamers in 1990 [25,26]. To date, numerous high affinity and highly specific aptamers have been identified against a broad range of targets such as metal ions, small organics, peptides, nucleic acids, proteins, viruses and whole cells

[27,28]. In particular, aptamers possess several significant advantages over antibodies including low molecular weight, high stability, ease of synthesis and modification, and rapid folding properties [29]. Thus aptamers are promising alternatives to antibodies in many different applications, especially bioanalytical applications [30-32]. However, to the best of our knowledge, aptamers have not been reported for any GDH enzyme. Given the importance of GDH in the diagnosis of CDI and lack of anti-GDH aptamers for the development of potential aptamer-based tests for *C. difficile* detection, in this study we made an effort to develop anti-GDH DNA aptamers via in vitro selection. Here we report the selection and characterization of aptamers as high-affinity specific recognition receptors for GDH, as well as the engineering of a fluometric aptasensor for sensitive detection of GDH.

2. Materials and Methods

2.1 Chemicals and Reagents

All DNA oligonucleotides were obtained from Integrated DNA Technologies (IDT), and purified by standard 10% denaturing (8 M urea) polyacrylamide gel electrophoresis (dPAGE). The sequences of the random oligonucleotides and primers were as follows: DNA library, 5′-CAG GTC CAT CGA GTG GTA GGA-N_{40}-TCG CAC TGC TCC TGA ACG TAC-3′; forward primer (FP), 5’-CAG GTC CAT CGA GTG GTA GGA-3′; reverse primer 1 (RP1), 5′-GTA CGT TCA GGA GCA GTG CGA-3′; reverse primer 2 (RP2), 5′-AAA AAA AAA AAA/iSpC3/GTA CGT TCA GGA GCA GTG CGA-3′; FAM-labeled anti-GDH1-T1: 5′-FAM-TAG GAG GAG GTA TTT AGT GCC AAG CCA TCT CAA ACG ACG TCT GAG TCG CAC TGC TCC TG-3′. Two versions of GDH proteins were used in this study: recombinant (his-tagged) glutamate dehydrogenase (rGDH; expressed and purified from *E. coli* cells with isoelectric point of 5.60), and native GDH (nGDH; directly purified from *C. difficile* cells), both of which were obtained from Pro-Lab Diagnostics (Toronto, Canada). TcdA and TcdB proteins from *C. difficile* were also provided by Pro-Lab Diagnostics. Human immunoglobulin G (IgG) and human thrombin were obtained from Sigma. *Thermus thermophilus* DNA polymerase was obtained from Biotools. γ-[^{32}P]-ATP was purchased from Perkin Elmer. Adenosine 5′-triphosphate (ATP),

dNTPs and T4 polynucleotide kinase (PNK) were purchased from MBI Fermentas. Ni-NTA magnetic agarose beads were obtained from QIAGEN. All other chemicals and solvents were purchased from Sigma and used without further purification. Water was purified with a Milli-Q Synthesis A10 water purification system.

2.2 Characterization

Time-dependent fluorescence emission measurements were performed using a Cary Eclipse fluorescence spectrophotometer (Varian) with an excitation wavelength of 494 nm and emission wavelength of 518 nm. The bandpasses for excitation and emission were set at 5 nm/5 nm and photomultiplier tube voltage was 600 V. Fluorescence data was typically collected every 1 min over a period of 60 min. Both the phosphorimage and fluorimage of gels were obtained using a Typhoon 9200 variable mode imager (GE Healthcare) and analyzed by ImageQuant software (Molecular Dynamics).

2.3 *In vitro* selection of aptamers

The SELEX procedure was performed according to a previously reported method with minor modifications [33], and is shown in Figure 1. rGDH-bound Ni-NTA magnetic beads were first prepared by incubating 100 μL of a 5% (w/v) suspension of Ni-NTA magnetic agarose beads (Qiagen) and 10 μL of rGDH (2.3 mg/mL) in 1× binding buffer (1× PBS, containing 150 mM NaCl and 0.02% Tween-20, pH 7.6) with a final volume of 500 μL. After mixing with rotation for 1 h at 4 °C, the rGDH-coated beads were washed three times with binding buffer, re-suspended and stored in 500 μL binding buffer at 4 °C.

For the initial round of SELEX, 20 μM of DNA library, which was denatured at 95 °C for 5 min and immediately cooled on ice for 10 min, was first counter-selected against 20 μL of a 5% suspension of Ni-NTA magnetic beads in 500 μL of 1× binding buffer in order to reduce non-specifically bound DNA molecules. Then the remaining unbound DNA library was exposed to 100 μL of bead-bound rGDH with rotation in 500 μL 1× binding buffer at room temperature. After incubating for 30 min, the beads were magnetically trapped and washed three times with binding buffer to remove the unbound DNA. Subsequently, target-bound aptamers were eluted by incubating the recovered beads with 300 μL of

elution buffer (1× binding buffer containing 500 mM imidazole) at 37 °C for 20 min with gentle shaking. After recovery by ethanol precipitation, the obtained DNA was amplified by PCR1. Each PCR mixture (50 μL) contained the DNA template prepared above, 1 μM FR, 1 μM RP1, 200 μM dNTPs, 1× PCR reaction buffer (75 mM Tris-HCl, pH 9.0, 2 mM $MgCl_2$, 50 mM KCl, 20 mM $(NH_4)_2SO_4$) and 2.5 U *Thermus thermophilus* DNA polymerase. Thermal cycles were typically performed as follows: 94 ºC for 30 s; 16 cycles of 94 ºC for 30 s, 50 ºC for 45 s and 72 ºC for 40 s; 72 ºC for 5 min. An agarose gel (3%) electrophoresis was performed to check the PCR1 product. In order to separate the relevant DNA strands from the double-stranded PCR1 products, the above PCR1 product was used as the template for PCR2 using primers FR and RP2 while following the same protocol as for PCR1. During this process, the hexaethyleneglycol spacer in RP2 can prevent the amplification of the A_{12} fragment, thus making the nonaptamer-coding DNA strand 12 nucleotides longer than the coding strand. The DNA aptamers were separated and purified by 10% dPAGE (8 M urea), and used as the ssDNA library for the next round. After 10 rounds of selection, 100 nM of purified PCR1 product that contained a unique 6 nt barcode was subjected to deep sequencing using the MiSeq (Illumina) sequencing platform.

2.4 Identification of High-Affinity Aptamers for rGDH

To evaluate the binding characteristics of all sequenced aptamers, we performed the SELEX procedure as described above. Briefly, the aptamer candidates were first labeled with γ-[^{32}P]-ATP at the 5′ end by using T4 polynucleotide kinase according to the manufacturer's protocol, and purified by 10% dPAGE (8 M urea). Then 100 nM aptamer candidate was incubated with 100 μL rGDH-coated beads at room temperature for 30 min in a total volume of 500 μL 1× binding buffer with gentle rotation. In parallel, negative controls consisting of the aptamer incubated with uncoated beads were included. Following several washing steps, the bound ssDNA in the reaction mixtures were analyzed by 10% dPAGE.

To determine the binding affinity of identified aptamers towards rGDH, binding assays were conducted in 500 μL of 1× binding buffer containing a fixed number of bead-bound rGDH (100 μL) and radioactively-labeled aptamers in a range of concentrations (0 nM to 100 nM). Uncoated beads were

used as a negative control for nonspecific binding in each experiment. The apparent dissociation constants (K_d) of each aptamer were obtained by fitting the fractional bound DNA to the total aptamer concentration using a one-site binding model.

2.5 Electrophoretic mobility shift assays (EMSA)

Binding reactions were performed in 20 μL of 1× binding buffer containing 3 nM ^{32}P-labeled anti-GDH1-T1 aptamer and various concentrations of rGDH (0 to 1000 nM). After incubation for 30 min, the reaction mixtures were spiked with 6× loading buffer, and then loaded into the wells of a non-denaturing polyacrylamide gel (8%) at 4 °C. Visualization of DNA bands was done using a Typhoon 9200 imager and the resulting bands were quantified with ImageQuant software.

2.6 Procedure for nGDH Assay

In a typical assay, 20 μL of 5× binding buffer (5× PBS, containing 750 mM NaCl and 0.1% Tween-20, pH 7.6), 2 μL of FAM-labeled (5′ end) aptamer probe (7 μM), 30 μL of reduced graphene oxide (RGO) solution (100 μg/mL) and 48 μL of water were first mixed and incubated in a micro-centrifuge tube for 30 min. Then, 10 μL of 1% BSA was added to block the surface. After incubating for 20 min, 5 μL of nGDH with different dilutions was added to the mixture and time-dependent fluorescence emission measurements were performed at λ_{ex} /λ_{em} = 494/518 nm. The emission intensity obtained at a reaction time of 60 min was plotted against nGDH concentration to obtain a limit of detection. A similar experiment was carried out using non-target proteins (BSA, human thrombin, human IgG, TcdA and TcdB from *C. difficile*) to evaluate aptamer selectivity.

3. Results and Discussion

GDH testing has been used as an effective diagnostic tool for CDI, with a negative predictive value as high as 99% [14,17,18]. In the current study, using recombinant GDH (rGDH; the *C. difficile* GDH expressed and purified from *E. coli*) as a target, we performed the SELEX method to identify short synthetic DNA aptamers that could selectively bind this target with high affinity. The overall SELEX process is illustrated in Figure 1. The initial ssDNA library contained a central random sequence of 40

nucleotides (N_{40}) flanked on each side by a constant sequence of 21 nucleotides that can function as primer binding sites for PCR. rGDH (46.8 KDa) containing a C-terminal $(His)_6$-tag was immobilized onto Ni-NTA magnetic beads to yield a selection matrix. To eliminate the non-specific DNA, the denatured DNA pool was first exposed to bare magnetic beads. In this counter-selection, DNA molecules that bound to beads were separated and discarded. The unbound DNA molecules were then collected and incubated with the selection matrix. After removal of the unbound sequences, the rGDH-bound DNA were eluted and amplified by PCR. The sense DNA was separated and purified by gel electrophoresis due to the fact that PCR products contained a primer with a spacer and an extension of 12 nucleotides. The recovered DNA (~ 100 pmol) was then used as input DNA for the next round of selection. A total of 10 selection rounds were completed, after which we analyzed the sequences from the DNA pools by high-throughput sequencing.

The sequencing results indicated an enrichment of aptamer candidate sequences. The total number of sequencing reads was about 6 million. Among these, the top 10 highest multiplicity sequences for rGDH represented 17% of the selected pools (Table S1). To rapidly identify the selected sequences with high affinities, we labeled each of the 10 sequenced aptamer candidates with γ-[^{32}P]-ATP, and tested each for its ability to bind to rGDH immobilized on magnetic beads using the original SELEX conditions. Binding assays carried out for each sequence against uncoated beads were used as negative controls. As shown in Figure 2A, the initial DNA library did not yield any obvious signal above background levels (S/B). However, anti-GDH1, anti-GDH3 and anti-GDH7 showed high binding affinity for rGDH. By performing rGDH binding assays we calculated the equilibrium dissociation constants (K_d) in the low nanomolar range (Figure 2B). The lowest K_d of 3.1 ± 1.2 nM was obtained for anti-GDH1. For anti-GDH3 and anti-GDH7, the K_d values were determined to be 5.6 ± 2.4 nM and 4.6 ± 1.6 nM, respectively. These affinities were in accordance with previous studies on aptamers targeting diverse proteins, such as thrombin [34], PDGF [35], IgE [36], and streptavidin [37], with K_d values in the low nanomolar range. To understand the structural differences between the aptamers, we estimated the

theoretical secondary structures using a dynamic programming algorithm of lowest free energy [38]. Typical stem-loop motifs were found in their secondary structures (Figure S1).

It is well-known that not all of the nucleotides play an important role in the aptamer-target binding reaction. An aptamer usually contains nucleotides that either bind to the target or facilitate the binding [39]. To determine the key nucleotides in the anti-GDH aptamer, truncated versions were produced based on the secondary structure of the anti-GDH1 aptamer, in which stem-loop structure (I) at the 5′ end and a non-pairing region at the 3′ end were removed to yield the 59 nucleotide variant -T1. This variant could bound rGDH-coated beads with a bound percentage of 90 ± 4% (Figure S2), similar to the full-length aptamer. We further shortened T1 by deleting the primers region, leaving the random sequence of 40 nucleotides in variant T2. However, this truncation resulted in a significant loss of binding ability (10 ± 6%), implying that the stem formed between the random sequence and part of the primer region was essential for maintaining the binding conformation. Removing the G-rich part at the 5′ end of the T1 variant decreased the binding ability (T3; 78 ± 7%), indicating that the G-rich region could be of importance for protein binding through the formation of advanced tertiary structures. If we deleted the CCTG sequence at the 3′ end of T3, it was observed that this truncated version (T4) retained similar binding affinity for rGDH (70 ± 7%). However, further removal of the GCT sequence at the 3′ end of T4 causes a change in the secondary structure (T5) and decreased its binding affinity (56 ± 9%), indicating the primary role of the non-pairing region in T4 for binding. Furthermore, there was no obvious binding for T6 (4 ± 3%) if we deleted the overhanging motif at the 5′ end of T5. Strikingly, in construct T3 we deleted the non-pairing region to obtain variant T7. This resulted in the complete loss of the binding ability (5 ± 4%), confirming that the recognition between anti-GDH1 and rGDH was dominantly controlled by the non-pairing region in T3. Finally, we removed the entire motif II and closed the remaining loop in T3. It was observed that this variant lost its binding affinity to rGDH (3 ± 1%), suggesting that the terminal stem-loop section of T3 was critical for keeping the secondary structure for binding.

The truncated aptamer, anti-GDH-T1, was then radioactively labeled at the 5' end and tested for binding to the rGDH target by EMSA assays [40,41]. A typical image of an EMSA result is shown in Figure 3A. We observed that the electrophoretic mobility of the protein-aptamer complex was typically less than that of the free aptamer. The fractional saturation of bound aptamer was calculated as a function of rGDH concentration (Figure 3B). A K_d value of 4.5 ± 2.2 nM was determined for the anti-GDH1-T1 aptamer, indicating its high-affinity. The specificity was also tested by EMSA. No obvious band was observed when using proteins such as BSA, thrombin and IgG (Figure S3).

The anti-GDH1-T1 aptamer was then used to produce a fluorescence-based biosensor for detecting native GDH from *C. difficile* (nGDH). Biosensing by fluorescence has attracted much attention in the design of various aptasensors, largely due to its simplicity and sensitivity [42,43]. Our group has previously reported a structure-switching approach for engineering signaling aptamers that functioned by switching structures from DNA-DNA duplex to aptamer-target complex [44]. The presence of target triggers the release of a quencher-labeled complementary DNA strand from the fluorophore-labeled aptamer, accompanied by an increase of fluorescence intensity because of fluorescence dequenching. In spite of the general utility of the strategy, fine-tuning of the complementary DNA remains a major challenge as many sequences must be rationally designed and tested to make sure that the signaling aptamers undergo a significant conformational change upon target binding. Therefore, we sought to overcome this problem by coupling the aptamer to graphene-based nanomaterials, due to the fact that: (1) the π-rich conjugation domains allow graphene to directly interface with DNA through non-covalent π-π stacking interaction [45,46]; (2) graphene produces highly efficient fluorescence quenching based on energy transfer or electron transfer mechanisms [47,48].

The working principle and key functionalities of the aptamer-graphene biosensor are schematically illustrated in Figure 4A. Reduced graphene oxide (RGO) was used to reduce the background fluorescence signal [49]. First, the structure-switching signaling aptamer-graphene construct was obtained by non-covalent self-assembly of a fluorophore-labeled anti-GDH-T1 aptamer onto the surface of RGO in solution. Then the free sites in RGO were blocked by BSA in order to minimize the

nonspecific binding of GDH onto the RGO surface. Upon recognition and binding of specific targets by the adsorbed aptamers, the conformational switch of the bound aptamers occurred in conjunction with the desorption of the weakly binding aptamer-target complex from the RGO surface [50], which immediately recovered the fluorescence signal. Thus the target recognition event was efficiently converted into a measurable signal, providing a powerful analytical sensing system.

To validate the feasibility of the proposed sensing method, a kinetic study was carried out to record the time-dependent fluorescence changes of aptamers upon introduction of the GDH target (Figure 4B). As expected, the fluorescence intensity was initially quenched upon addition of the aptamer to RGO (it is noteworthy that an experiment with varying concentrations of RGO was conducted to ensure the complete fluorescence quenching of aptamers; see Figure S4). In direct contrast, when nGDH was added, the fluorescence intensity was restored, and increases as a function of reaction time. This result suggested a conformational change of the aptamer upon binding to target, which would weaken the interaction between the aptamer probe and RGO, thereby causing desorption and/or causing the fluorescence probe in weakly bound aptamers to move away from the RGO surface, hindering the energy transfer or electron transfer process. After 1 h incubation, a fluorescence enhancement of more than 14-fold was obtained.

Since graphenes can also function as a scaffold for binding protein through electrostatic interactions, hydrophobic interactions or aromatic π-π stacking [51], it was crucial to minimize the free surface binding sites to avoid the nonspecific binding of nGDH on RGO surface. With the aim of studying the effect of blocking agent on the sensor response, a treatment of the system was carried out with different concentrations of BSA. The signal response quantified as signal-to-background (S/B) ratios increased with increased amount of BSA from 0.05% to 0.5% (Figure S5). This result suggested that the blocking procedure was necessary to remove the unspecific binding sites on the RGO surface, thus improving the sensor sensitivity [52]. As noted, this method presented here could open new opportunities for improving the performance of graphene-aptamer based fluorescent biosensors [53-55].

To demonstrate the sensitivity of the proposed biosensor for the detection of nGDH, a kinetic study was carried out to record the time-dependent fluorescence changes upon the addition of various amounts of nGDH. As shown in Figure 4C, the kinetics of the fluorescence enhancement and the endpoint intensity (at 60 min) was dependent on the nGDH concentrations. The detection limit (defined as 3σ/slope, with σ being the standard deviation of the blank samples) of the sensor was determined to be 1 nM (Figure 5A). The selectivity of the aptamer-graphene biosensing system was also evaluated by using non-target proteins (BSA, thrombin, IgG, TcdA and TcdB). As shown in Figure 5B, no significant response was observed even when the concentration of each non-target protein was in 10-fold excess of nGDH, indicating the high selectivity of the developed aptasensor.

4. Conclusions

In summary, for the first time, anti-GDH DNA aptamers with high affinity and specificity were selected using SELEX technology. Furthermore, a structuring-switching signaling aptamer was developed through the direct non-covalent attachment of the aptamer to the surface of RGO, which enabled the real-time, sensitive and selective detection of GDH, thus making it a promising candidate for an initial GDH screening test in clinical diagnosis of CDI.

AUTHOR INFORMATION

Corresponding Authors

*liying@mcmaster.ca, brennanj@mcmaster.ca

ACKNOWLEDGMENT. Funding for this work was provided by the Natural Sciences and Engineering Council of Canada through a Collaborative Research and Development grant, the Ontario Ministry of Research and Innovation (through an Ontario Research Fund-Research Excellence grant), Pro-Lab Diagnostics and the Canadian Foundation for Innovation.

SUPPORTING INFORMATION PARAGRAPH. This material is available free of charge via the Internet at

References.

[1] B. Stoddart, M.H. Wilcox, Clostridium difficile, Curr. Opin. Infect. Dis. 15 (2002) 513-518.

[2] J.G. Bartlett, Clostridium difficile: history of its role as an enteric pathogen and the current state of knowledge about the organism, Clin. Infect. Dis. 18 (1994) 265-272.

[3] D.M. Lyerly, H.C. Krivan, T.D. Wilkins, *Clostridium difficile*: its disease and toxins, Clin. Microbiol. Rev. 1 (1988) 1-18.

[4] L.V. McFarland, W.E. Stamm, Review of *Clostridium difficile*-associated diseases, Am. J. Infect. Control 14 (1986) 99-109.

[5] D. Gravel, M. Miller, A. Simor, G. Taylor, M. Gardam, A. McGeer, J. Hutchinson, D. Moore, S. Kelly, D. Boyd, M. Mulvey, Canadian Nosocomial Infection Surveillance Program, Health care-associated *Clostridium difficile* infection in adults admitted to acute care hospitals in Canada: a Canadian Nosocomial Infection Surveillance Program Study, Clin. Infect. Dis. 48 (2009) 568-576.

[6] M. Rupnik, M.H. Wilcox, D.N. Gerding, *Clostridium difficile* infection: new developments in epidemiology and pathogenesis, Nat. Rev. Microbiol. 7 (2009) 526-536.

[7] R.P. Vonberg, C. Reichardt, M. Behnke, F. Schwab, S. Zindler, P. Gastmeier, Costs of nosocomial *Clostridium difficile*-associated diarrhea, J. Hosp. Infect. 70 (2008) 15-20.

[8] C.P. Kelly, J.T. LaMont, *Clostridium difficile* infection, Annu. Rev. Med. 49 (1998) 375-390.

[9] L.G. Arroyo, J. Rousseau, B.M. Willey, D.E. Low, H. Staempfli, A. McGeer, J.S. Weese, Use of a selective enrichment broth to recover *Clostridium difficile* from stool swabs stored under different conditions, J. Clin. Microbiol. 43 (2005) 5341-5343.

[10] L.R. Peterson, P.J. Kelly, H.A. Nordbrock, Role of culture and toxin detection in laboratory testing for diagnosis of *Clostridium difficile*-associated diarrhea, Eur. J. Clin. Microbiol. Infect. Dis. 15 (1996) 330-336.

[11] C.P. Kelly, C. Pothoulakis, J.T. LaMont, Clostridium difficile colitis, N. Engl. J. Med. 330 (1994) 257-262.

[12] T. Planche, A. Aghaizu, R. Holliman, P. Riley, J. Poloniecki, A. Breathnach, S. Krishna, Diagnosis of *Clostridium difficile* infection by toxin detection kits: a systematic review, Lancet Infect. Dis. 8 (2008) 777-784.

[13] F. Barbut, M. Braun, B. Burghoffer, V. Lalande, C. Eckert, Rapid detection of toxigenic strains of *Clostridium difficile* in diarrheal stools by real-time PCR, J. Clin. Microbiol. 47 (2009) 1276-1277.

[14] K.C Carroll, Tests for the diagnosis of *Clostridium difficile* infection: the next generation, Anaerobe 17 (2011) 170-174.

[15] N. Shetty, M.W.D. Wren, P.G. Coen, The role of glutamate dehydrogenase for the detection of *Clostridium difficile* in faecal samples: a meta-analysis, J. Hosp. Infect. 77 (2011) 1-6.

[16] S.D. Goldenberg, M. Gumban, A. Hall, A. Patel, G.L. French, Lack of effect of strain type on detection of toxigenic *Clostridium difficile* by glutamate dehydrogenase and polymerase chain reaction, Diagn. Microbiol. Infect. Dis. 70 (2011) 417-419.

[17] L. Zheng, S.F. Keller, D.M. Lyerly, R.J. Carman, C.W. Genheimer, C.A. Gleaves, S.J. Kohlhepp, S. Young, S. Perez, K. Ye, Multicenter evaluation of a new screening test that detects *Clostridium difficile* in fecal specimens, J. Clin. Microbiol. 42 (2004) 3837-3840.

[18] L. Fenner, A.F. Widmer, G. Goy, S. Rudin, R. Frei, Rapid and reliable diagnostic algorithm for detection of *Clostridium difficile*, J. Clin. Microbiol. 46 (2008) 328-330.

[19] S.D. Goldenberg, P.R. Cliff, S. Smith, M. Milner, G.L. French, Two-step glutamate dehydrogenase antigen real-time polymerase chain reaction assay for detection of toxigenic *Clostridium difficile*, J. Hosp. Infect. 74 (2010) 48-54.

[20] M. Kawada, M. Annaka, H. Kato, S. Shibasaki, K. Hikosaka, H. Mizuno, Y. Masuda, T. Inamatsu, Evaluation of a simultaneous detection kit for the glutamate dehydrogenase antigen and toxin A/B in feces for diagnosis of *Clostridium difficile* infection, J. Infect. Chemother. 17 (2011) 807-811.

[21] S.H. Cohen, D.N. Gerding, S. Johnson, C.P. Kelly, V.G. Loo, L.C. McDonald, J. Pepin, M.H. Wilcox, Society for Healthcare Epidemiology of America, Infectious Diseases Society of America, Clinical practice guidelines for *Clostridium difficile* infection in adults: 2010 update by the society for healthcare epidemiology of America (SHEA) and the infectious diseases society of America (IDSA), Infect. Control Hosp. Epidemiol. 31 (2010) 431-455.

[22] K. Eastwood, P. Else, A. Charlett, M. Wilcox, Comparison of nine commercially available *Clostridium difficile* toxin detection assays, a real-time PCR assay for *C. difficile tcdB*, and a glutamate dehydrogenase detection assay to cytotoxin testing and cytotoxigenic culture methods, J. Clin. Microbiol. 47 (2009) 3211-3217.

[23] F.C. Tenover, E.J. Baron, L.R. Peterson, D.H. Persing, Laboratory diagnosis of *Clostridium difficile* infection can molecular amplification methods move us out of uncertainty?, J. Mol. Diagn. 13 (2011) 573-582.

[24] T.D. Wilkins, D.M. Lyerly, *Clostridium difficile* testing: after 20 years, still challenging, J. Clin. Microbiol. 41 (2003) 531-534.

[25] C. Tuerk, L. Gold, Systematic evolution of ligands by exponential enrichment: RNA ligands to bacteriophage T4 DNA polymerase, Science 249 (1990) 505-510.

[26] A.D. Ellington, J.W. Szostak, *In vitro* selection of RNA molecules that bind specific ligands, Nature 346 (1990) 818-822.

[27] S.M. Shamah, J.M. Healy, S.T. Cload, Complex target SELEX, Acc. Chem. Res. 41 (2008) 130-138.

[28] E.J. Cho, J.W. Lee, A.D. Ellington, Applications of aptamers as sensors, Annu. Rev. Anal. Chem. 2 (2009) 241-264.

[29] M. Mascini, I. Palchetti, S. Tombelli, Nucleic acid and peptide aptamers: fundamentals and bioanalytical aspects, Angew. Chem. Int. Ed. 51 (2012) 1316-1332.

[30] C.L.A. Hamula, J.W. Guthrie, H.Q. Zhang, X.F. Li, X.C. Le, Selection and analytical applications of aptamers, TrAC-Trend Anal. Chem. 25 (2006) 681-691.

[31] K. Sefah, J.A. Phillips, X.L. Xiong, L. Meng, D.Van Simaeys, H. Chen, J. Martin, W.H. Tan, Nucleic acid aptamers for biosensors and bio-analytical applications, Analyst 134 (2009) 1765-1775.

[32] A.B. Iliuk, L. Hu, W.A. Tao, Aptamer in bioanalytical applications, Anal. Chem. 83 (2011) 4440-4452.

[33] A. Allali-Hassani, M.P. Pereira, N.K. Navani, E.D. Brown, Y.F. Li, Isolation of DNA aptamers for CDP-ribitol synthase, and characterization of their inhibitory and structural properties, ChemBioChem 8 (2007) 2052- 2057.

[34] D.M. Tasset, M.F. Kubik, W. Steiner, Oligonucleotide inhibitors of human thrombin that bind distinct epitopes, J. Mol. Biol. 272 (1997) 688-698.

[35] L.S. Green, D. Jellinek, R. Jenison, A. Ostman, C.H. Heldin, N. Janjic, Inhibitory DNA ligands to platelet-derived growth factor B-chain, Biochemistry 35 (1996) 14413-14424.

[36] S.D. Mendonsa, M.T. Bowser, In vitro selection of high-affinity DNA ligands for human IgE using capillary electrophoresis, Anal. Chem. 76 (2004) 5387-5392.

[37] S.S. Oh, K.M. Ahmad, M. Cho, S. Kim, Y. Xiao, H.T. Soh, Improving aptamer selection efficiency through volume dilution, magnetic concentration, and continuous washing in microfluidic channels, Anal. Chem. 83 (2011) 6883-6889.

[38] A.R. Gruber, R. Lorenz, S.H. Bernhart, R. Neuböck, I.L. Hofacker, The Vienna RNA websuite, Nucleic Acids Res. 36 (2008) W70-W74.

[39] D.J. Galas, A. Schmitz, DNAase footprinting a simple method for the detection of protein-DNA binding specificity, Nucleic Acids Res. 5 (1978) 3157-3170.

[40] L.M. Hellman, M.G. Fried, Electrophoretic mobility shift assay (EMSA) for detecting protein-nucleic acid interactions, Nat. Protoc. 2 (2007) 1849-1861.

[41] M.J. Ferber, L.J. Maher, Quantitating oligonucleotide affinities for duplex DNA: footprinting vs electrophoretic mobility shift assays, Anal. Biochem. 244 (1997) 312-320.

[42] R. Nutiu, Y. Li, Structure-switching signaling aptamers: transducing molecular recognition into fluorescence signaling, Chem. Eur. J. 19 (2004) 1868-1876.

[43] R. Nutiu, Y. Li, Aptamers with fluorescence-signaling properties, Methods 37 (2005) 16-25.

[44] R. Nutiu, Y. Li, Structure-switching signaling aptamers, J. Am. Chem. Soc. 125 (2003) 4771-4778.

[45] N. Varghese, U. Mogera, A. Govindaraj, A. Das, P.K. Maiti, A.K. Sood, C.N. Rao, Binding of DNA nucleobases and nucleosides with graphene, ChemPhysChem 10 (2009) 206-210.

[46] B. Liu, S. Salgado, V. Maheshwari, J. Liu, DNA adsorbed on graphene and graphene oxide: fundamental interactions, desorption and applications, Curr. Opin. Colloid Interface Sci. 26 (2016), 41-49.

[47] R.S. Swathi, K.L. Sebastian, Resonance energy transfer from a dye molecule to graphene, J. Chem. Phys. 129 (2008) 054703.

[48] K.P. Loh, Q. Bao, G. Eda, M. Chhowalla, Graphene oxide as a chemically tunable platform for optical applications, Nat. Chem. 2 (2010) 1015-1024.

[49] C. Lu, P.J. Huang, B. Liu, Y. Ying, J. Liu, Comparison of graphene oxide and reduced graphene oxide for DNA adsorption and sensing, Langmuir 32 (2016) 10776-10783.

[50] Y. Wang, Z.H. Li, D.H. Hu, C.T. Lin, J.H. Li, Y.H. Lin, Aptamer/graphene oxide nanocomplex for *in situ* molecular probing in living cells, J. Am. Chem. Soc. 132 (2010) 9274-9276.

[51] S.S. Chou, M. De, J. Luo, V.M. Rotello, J. Huang, V.P. Dravid, Nanoscale graphene oxide (nGO) as artificial receptors: implications for biomolecular interactions and sensing, J. Am. Chem. Soc. 134 (2012) 16725-16733.

[52] B. Liu, P.J. Huang, E.Y. Kelly, J. Liu, Graphene oxide surface blocking agents can increase the DNA biosensor sensitivity, Biotechnol. J. 11 (2016) 780-787.

[53] C.H. Lu, H.H. Yang, C.L. Zhu, X. Chen, G.N. Chen, A graphene platform for sensing biomolecules, Angew. Chem. Int. Ed. 48 (2009) 4785-4787.

[54] H. Pei, J. Li, M. Lv, J. Wang, J. Gao, J. Lu, Y. Li, Q. Huang, J. Hu, C. Fan, A graphene-based sensor array for high-precision and adaptive target identification with ensemble aptamers, J. Am. Chem. Soc. 134 (2012) 13843-13849.

[55] Y. Wang, Z. Li, J. Wang, J. Li, Y. Lin, Graphene and graphene oxide: biofunctionalization and applications in biotechnology, Trends Biotechnol. 29 (2011) 205-212.

FIGURE CAPTIONS.

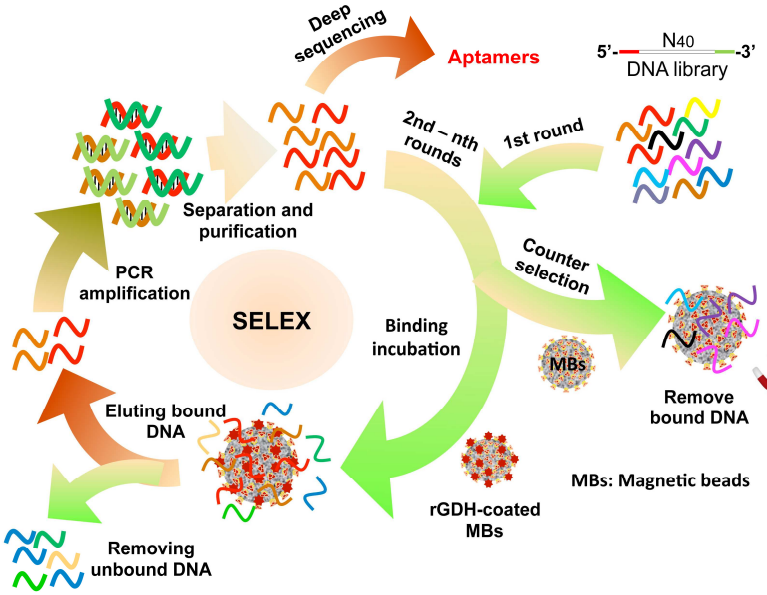

Figure 1. Schematic illustration of the aptamer selection procedure.

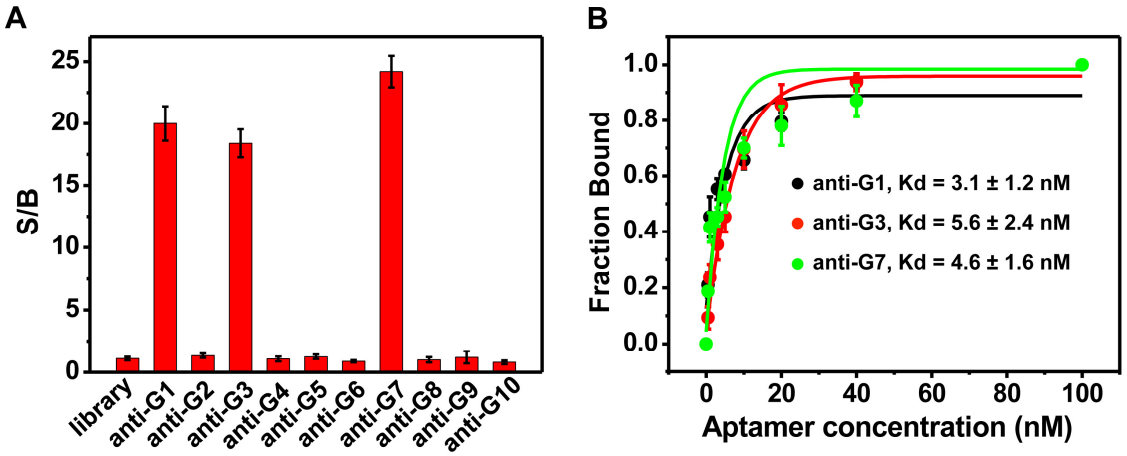

Figure 2. (A) Binding affinity assay to identify aptamer sequences. The signal-to-background ratio (S/B) was defined as S/B = I_1/I_0, where I_1 and I_0 were the measured radioactive signal in the presence and absence of target rGDH. (B) Determination of the dissociation constants (K_d) for the identified aptamers against rGDH. The fraction of radioactivity in the shifted DNA band is calculated and plotted against the concentration of protein.

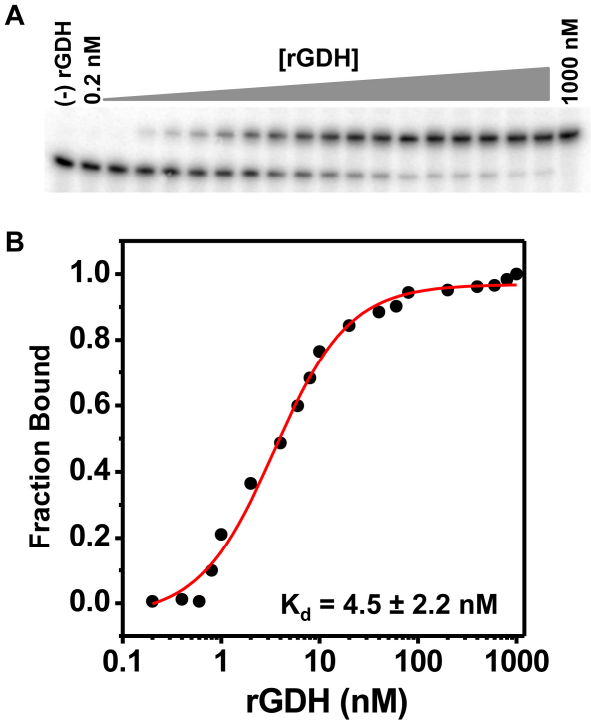

Figure 3. (A) Typical EMSA result for anti-GDH1-T1 aptamer binding to rGDH, and the corresponding binding curve (B).

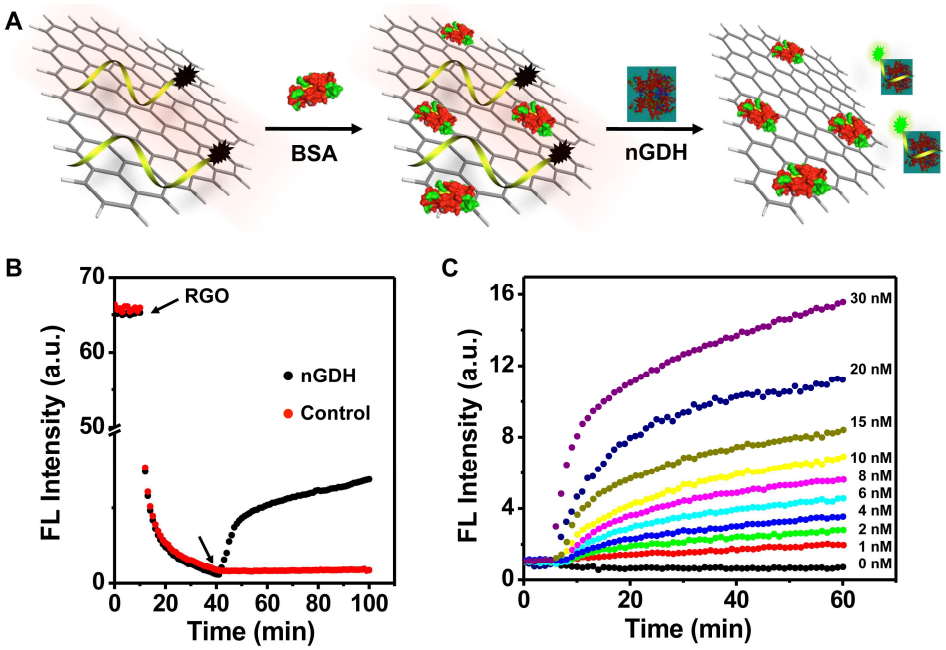

Figure 4. Functionalization of RGO with aptamers. (A) Schematic illustration of the RGO-aptamer system for nGDH detection. (B) The kinetic response of RGO-aptamer sensor to sequential addition of 30 μg/mL RGO and nGDH (100 nM) in binding buffer. (C) Time-dependent fluorescence response with varying concentrations of nGDH. $\lambda_{ex}/\lambda_{em}$ = 494/518 nm.

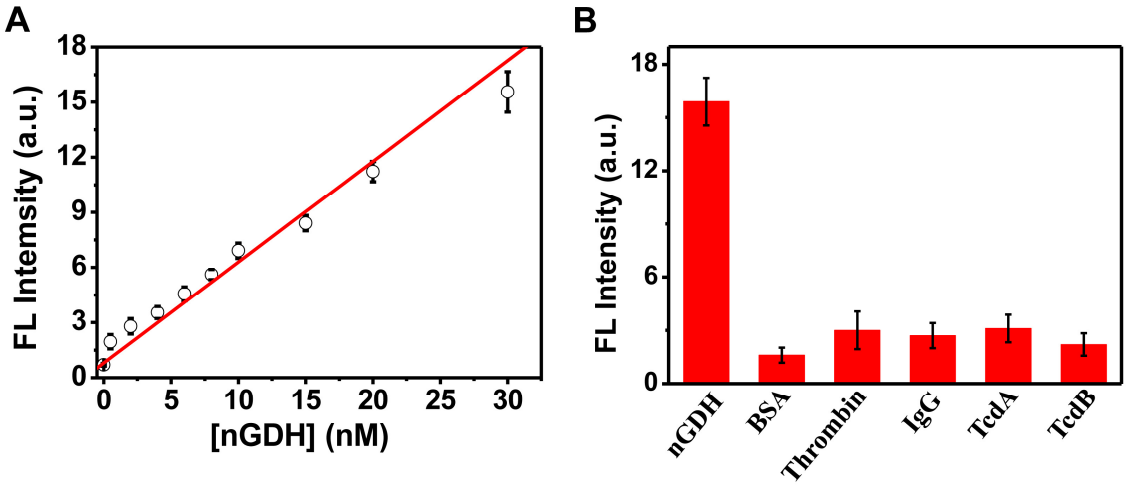

Figure 5. (A) Calibration curve of the aptasensor. The curve was plotted with the fluorescence intensity *vs* nGDH concentration. (B) Selectivity of the sensor for nGDH over other non-targeted proteins. The concentration of nGDH was 30 nM, and others were 300 nM each. The error bars represent the standard deviations of three parallel tests.

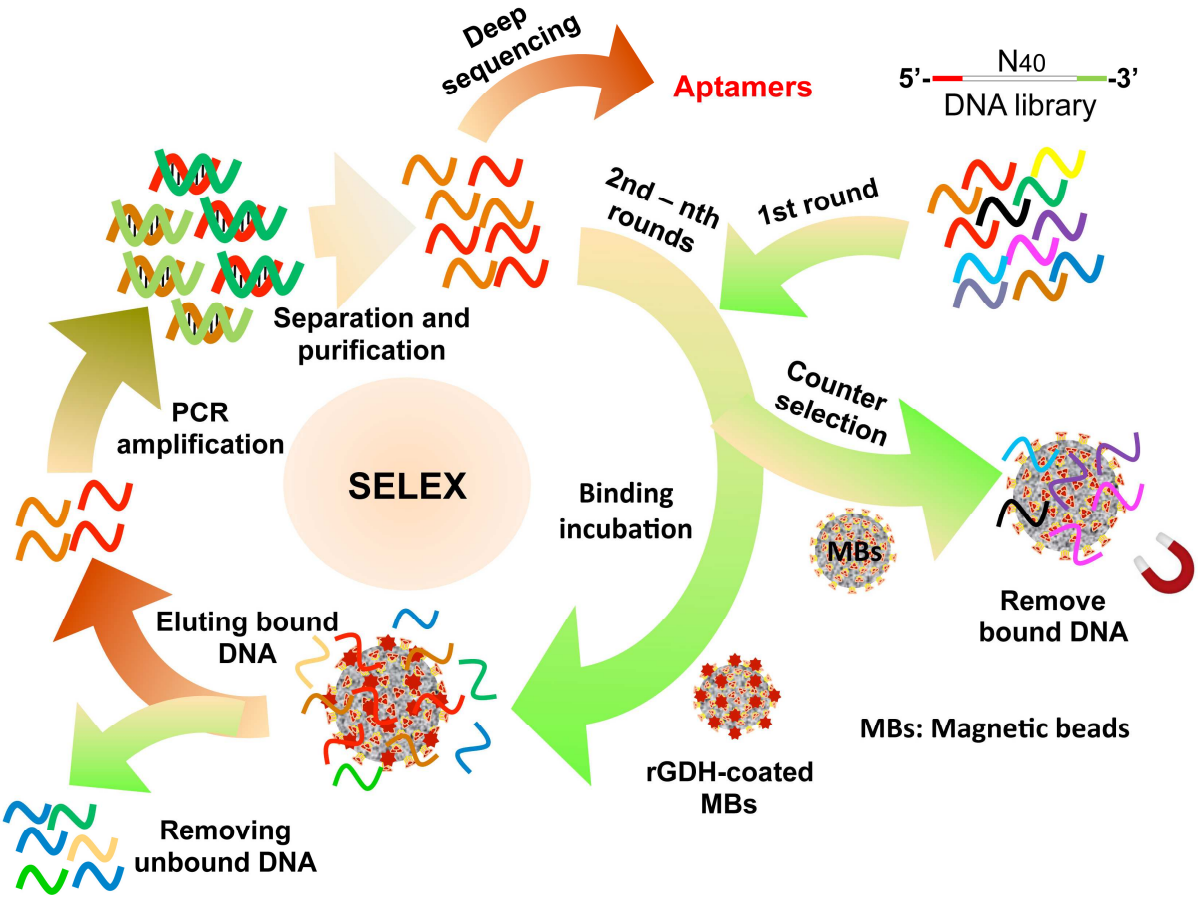

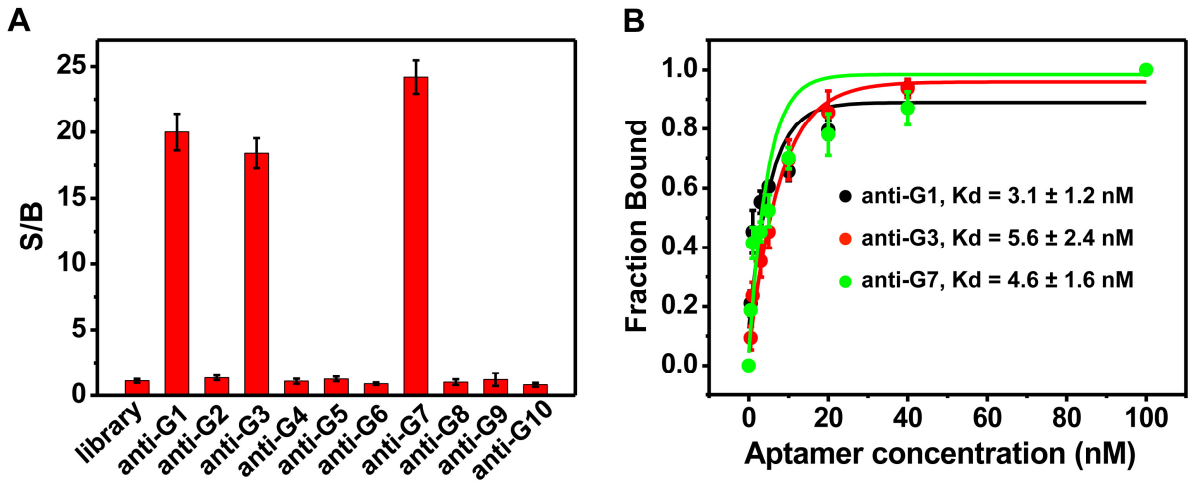

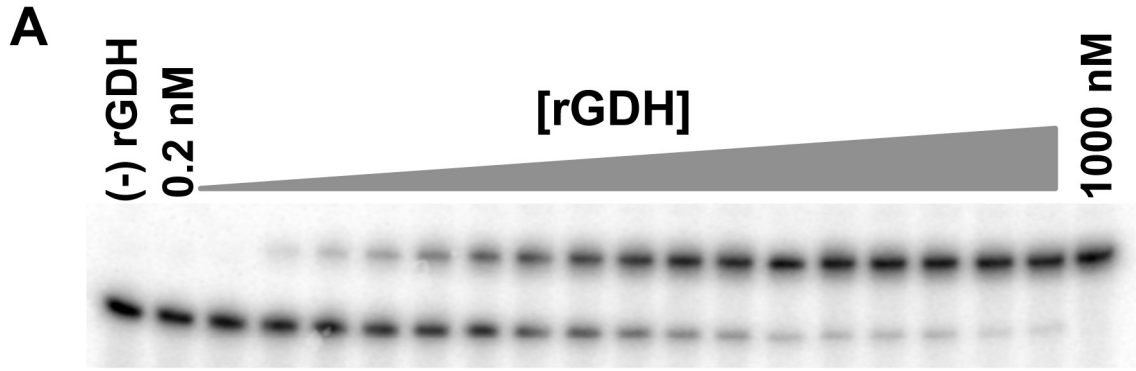
A
(-) rGDH
0.2 nM
[rGDH]
1000 nM

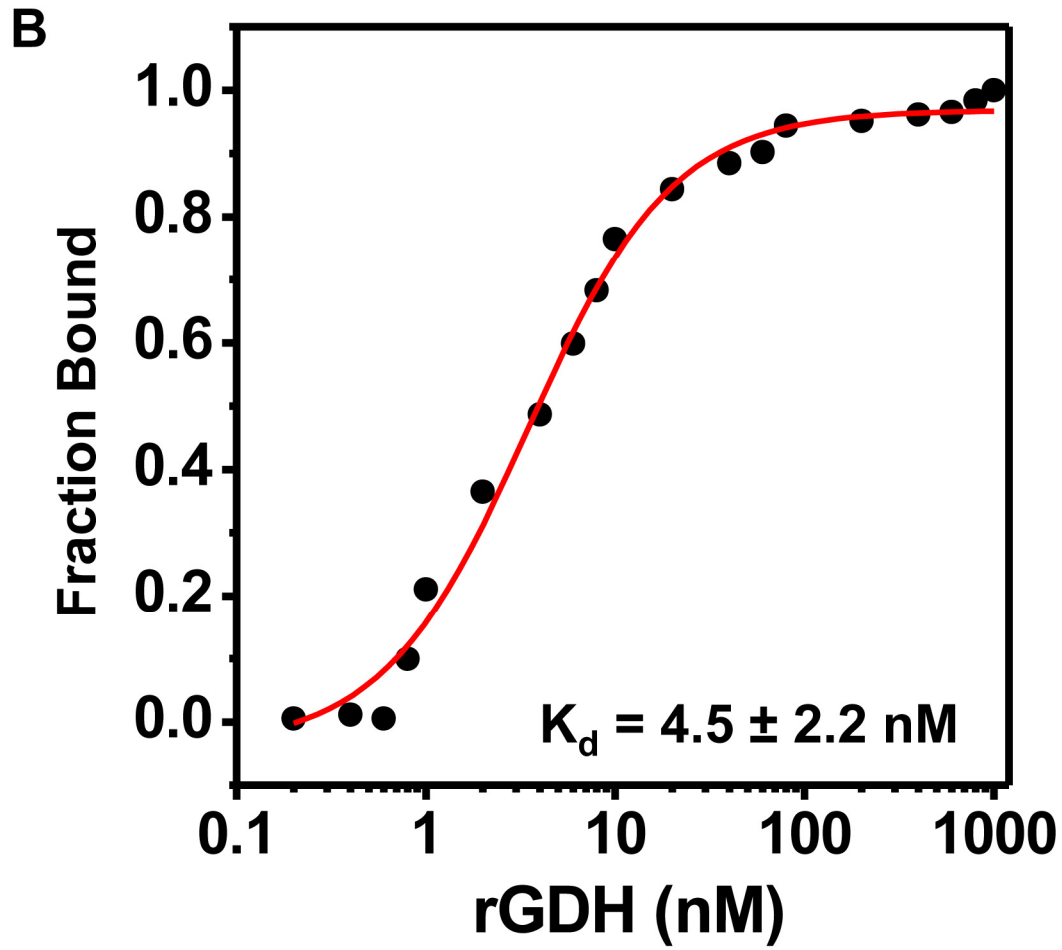
B
Fraction Bound
1.0
0.8
0.6
0.4
0.2
0.0
K_d = 4.5 ± 2.2 nM
0.1
1
10
100
1000
rGDH (nM)

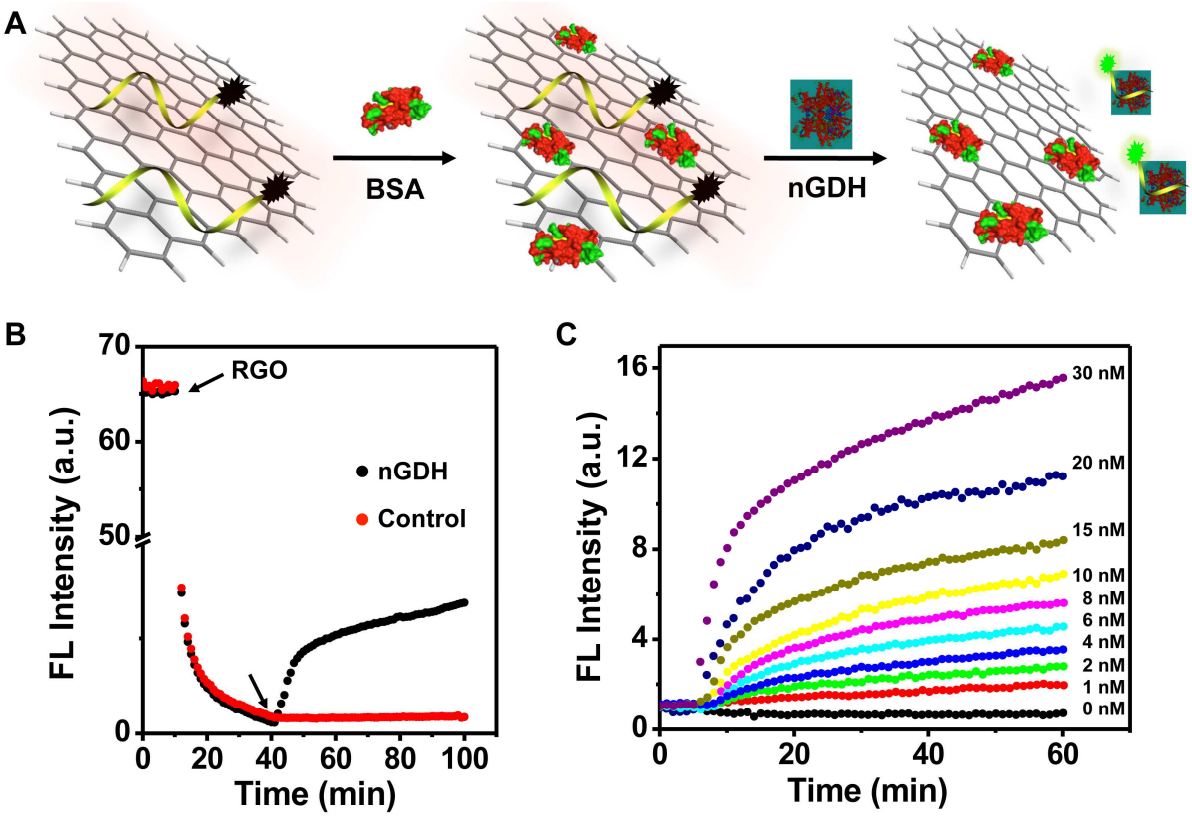

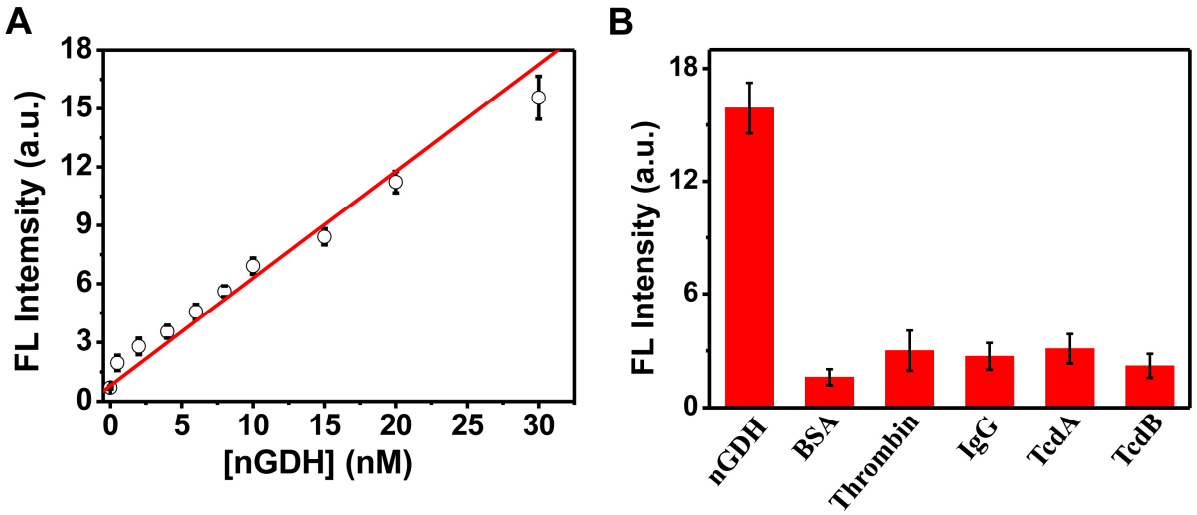

1. DNA aptamers were isolated from a random-sequence DNA pool to recognize glutamate dehydrogenase (GDH) from *Clostridium difficile* bacterium.
2. Three anti-GDH DNA aptamers with high affinity and specificity were identified.
3. A structuring-switching aptamer sensor was developed for the detection of GDH.